HHS Public Access

Author manuscript

Nature. Author manuscript; available in PMC 2014 February 27.

Published in final edited form as:

Nature. 2013 July 11; 499(7457): 228–232. doi:10.1038/nature12214.

Wnt activation in nail epithelium couples nail growth to digit regeneration

Makoto Takeo[1], **Wei Chin Chou**[1], **Qi Sun**[1], **Wendy Lee**[1], **Piul Rabbani**[1], **Cynthia Loomis**[1], **M. Mark Taketo**[2], and **Mayumi Ito**[1,*]

[1]The Ronald O. Perelman Department of Dermatology and the Department of Cell Biology New York University, School of Medicine, New York, NY 10016, USA

[2]Department of Pharmacology, Graduate School of Medicine, Kyoto University, Kyoto, 606-8501, Japan

Mammalian digit-tip can regenerate upon amputation[1,2], like amphibians. It is unknown why this capacity is limited to the area associated with the nail[2–4]. Here, we show that nail stem cells (NSCs) reside in the proximal nail matrix and that the mechanisms governing NSC differentiation are directly coupled with their ability to orchestrate digit regeneration. Early nail progenitors undergo Wnt-dependent differentiation into the nail. Upon amputation, this Wnt activation is required for nail regeneration and also for attracting nerves that promote mesenchymal blastema growth, leading to the regeneration of the entire digit. Amputations proximal to the Wnt-active nail progenitors result in the failure to regenerate the nail/digit (Supplementary Fig. S1). Nevertheless, β-catenin stabilization in the NSC region induced their regeneration. These results establish a link between NSC differentiation and digit regeneration, suggesting a utility of the NSCs in developing novel treatments for amputees.

Digit tip regeneration seen in both mice and humans involves the coordinated re-growth of the nail organ, including nail epithelial cells, and the terminal phalanx. Upon regrowth of the nail after amputation of the digit tip, undifferentiated mesenchymal cells including fate-restricted progenitor cells[5,6] accumulate under the wound epithelium and form the so-called blastema[7]. Growth and differentiation of these mesenchymal cells leads to digit regeneration. However, neither nail nor digit regenerates when amputated proximally to the nail[2–4,8,9] (Supplementary Fig. S2) and it is unknown why this limitation exists. Previous studies showed that nail transplantation following proximal digit amputation can induce ectopic digit bone differentiation[4], leading to a hypothesis that the nail epithelium has a

*Correspondence and requests for materials should be addressed to M.I. (Mayumi.Ito@nyumc.org).

Supplementary Information is linked to the online version of the paper at www.nature.com/nature.

The authors declare no competing financial interests.

Author contributions

M.T. designed and performed experiments, interpreted data and wrote the manuscript. W.C., P.R. and Q.S. performed experiments and interpreted data. M.M.T. generated β-catenin$^{fl/ex3}$ mice and interpreted the data. C.L. and W.L. interpreted data. M.I. designed experiments, interpreted data and wrote the manuscript.

special function in digit regeneration. Testing this hypothesis may provide an understanding of why regeneration is limited to the nail-associated part of digits, and how epithelial cells can influence underlying mesenchymal cells to regenerate digit bone. The role of the nail epithelium in digit regeneration has remained elusive, due in part to the lack of lineage and molecular analyses of normal nail epithelium.

To locate NSCs, we performed lineage tracing using *K14-creER; R26R-lacZ* reporter mice. A single injection of tamoxifen (TAM) genetically labeled a small subset of $K14^+$ nail basal epidermal cells, including nail matrix cells and bed cells, with LacZ (Fig. 1b, c). Over time, descendants of the labeled $K14^+$ nail epithelial cells extended linearly and distally, reflecting the direction of their growth (Fig. 1b). By 3 months after labeling, the number of $LacZ^+$ streaks emanating from the distal part of matrix and the bed decreased significantly (Fig. 1d). In contrast, the streaks emerging from the proximal matrix persisted for at least 5 months (Fig. 1b, d). These streaks included the proximal matrix, distal matrix and bed cells (Fig. 1e). The progeny of proximal matrix and distal matrix both migrated vertically to give rise to individual keratinized layers of the nail plate[10]. These results show that the proximal matrix contains self-renewing NSCs that sustain nail growth. $LacZ^+$ colonies in the nail fold, the epithelium surrounding the nail, were discontinuous from the streaks that gave rise to the nail plate, suggesting that the nail fold did not contribute to the cells for nail growth (Supplementary Fig. S4).

Histological analyses revealed that proximal matrix cells possessed less interdigitations, characteristic of undifferentiated epidermal cells (Supplementary Fig. S3). Immunohistochemistry with proliferation and epidermal differentiation markers[11] found that proximal matrix cells containing NSCs were highly proliferative ($Ki67^{high}$) and expressed K17 in addition to K14 (Supplementary Fig. S3). Isolated proximal matrix cells, enriched with $K14^+K17^+$ expression (Fig. 1f, g), exhibited the highest colony forming ability *in vitro*, a general characteristic of epithelial stem cells (Fig. 1h–j).

To understand molecular mechanisms underlying NSC differentiation, we generated a microarray of proximal matrix versus distal matrix. Most strikingly, the analyses revealed that proximal matrix cells enriched with NSCs downregulated Wnt signaling pathway genes, which is known to regulate embryonic development of limb/nail organ[12–14] as well as differentiation of epithelial and melanocyte stem cells[15]. Analyses with Wnt reporter mice showed that *Axin2-LacZ* signal started from the distal part of the $K17^+$ NSC region and persisted into the distal matrix, whereas the *TOPGAL* signal was seen in the $K17^-$ distal matrix[17,18]. Although these two markers distribute differently[16], both signals were absent in the proximal end of the nail matrix (Supplementary Fig. S5). Additionally, TCF1, a nuclear mediator of Wnt signaling[19], and *Wntless* (*Wls*), required for Wnt ligand secretion[20], were missing in the proximal end of the matrix. Moreover, several keratins that contained a *Tcf-1/Lef-1* consensus binding site were upregulated in the distal matrix compared with NSC region (Supplementary Table 1)[21,22], suggesting direct involvement of Wnt signaling in nail differentiation.

To verify the role of Wnt activation in the nail epithelium, we deleted β-catenin, an essential mediator of Wnt signaling, in adult epithelium using *K14-CreER;β-catenin*$^{fl/fl}$ (cKO) mice

(Fig. 2a). By two months after induction of β-catenin deletion by TAM treatment, nail formation is abrogated (Fig. 2b–e), as revealed by the lack of AE13, a marker for keratinized nail cells[22] (Fig. 2f). Moreover, the entire nail epithelium showed characteristics of the NSC region ($K17^{+}Ki67^{high}$) (Fig. 2g–i). Similar defects were observed in another mouse model (*K14-CreER;Wntless*$^{fl/fl}$) that depletes *Wls* in epithelial cells, confirming the essential role for Wnt signaling in nail differentiation (Supplementary Fig. S6).

Next, to determine how nail differentiation is linked to digit regeneration upon amputation, we treated cKO mice with TAM beginning immediately after digit amputation (Fig. 3a). We focused on digit bone regeneration to evaluate the completeness of the regenerative response since muscle and tendon are absent at this amputation level[6]. In control mice, the nail resumed its original structure by 5 weeks after amputation (Fig. 3b), and the amputated digit bone regenerated along with nail regeneration (Fig. 3c–f). In cKO mice, the nail failed to regenerate as expected due to the essential role for Wnt signaling in nail differentiation (Fig. 3b, e). Remarkably, bone regeneration in these mice was also completely blocked (Fig. 3c, d, f). Intact non-amputated digits in cKO mice (internal control) maintained similar digit bone length compared with intact digits in control mice at 5 weeks after TAM treatment (Fig. 3f).

Time-course studies showed that β-catenin was clearly depleted in nail epithelial cells of cKO mice by one week after TAM induction (Supplementary Fig. S7). Nonetheless, the amputated areas of both control and cKO mice were similarly re-epithelialized two weeks after amputation. In control mice, the regenerating nail matrix displayed Wnt activation with *TOPGAL* activity (Fig. 3g), contiguous with the original nail matrix cells, which permitted nail differentiation. Underneath the Wnt-active regenerating matrix, mesenchymal cells were actively proliferating (Fig. 3i). We identified that the majority (about 90%) of these proliferating cells express Runx2[23], a marker for osteoblast commitment (Supplementary Fig. S8), supporting previous notions that lineage-restricted progenitor cells contribute to the digit bone regeneration[5,6]. In cKO mice, however $Runx2^{+}$ progenitors and Sp7+ osteoblasts were not induced to proliferate, and the expression of *Bmp4*, functionally critical for digit bone regeneration[8], was missing in cKO digits (Supplementary Fig. S8). Furthermore, nerves that are vital for regeneration of rodent digits[24] and amphibian limbs[25] are located in the proliferative $Runx2^{+}$ mesenchyme close to the Wnt-active nail epithelial cells in control mice, whereas nerves did not extend to the regeneration area close to the epithelium in cKO mice (Fig. 1h, Supplementary Fig. S9). Moreover, Semaphorin 5a (Sema5a), an axon guidance molecule[26], is upregulated in control nail epithelium at 3 weeks after amputation, but not in that of cKO (Supplementary Fig. S10). This may suggest that nerves are attracted to paracrine factor(s) secreted from the Wnt-active nail epithelium, reminiscent of the ability of Wnt-active epithelium to attract nerves, as in the embryonic epidermis[27].

To investigate how Wnt-dependent innervations can promote digit regeneration, we surgically removed nerves before amputation. We then found a suppression of blastema growth similar to that in cKO mice (Supplementary Fig. S11). Subsequent microarray analysis showed that fibroblast growth factor (FGF) signaling was significantly downregulated in denervated digits at 3 weeks after amputation when blastema grows in control digits (data not shown). This is particularly interesting, given the vital roles of FGF

signaling during amphibian limb regeneration[28]. Immunostaining confirmed that FGF2 was induced in a distal area of regenerating nail epithelium by 3 weeks after amputation (Supplementary Fig. S12). In contrast, FGF2 was not expressed in the nail epithelium of denervated digits (Supplementary Fig. S12). Notably, cKO mice that showed deficient innervations in the blastema also lacked FGF2 expression in the nail epithelium (Supplementary Fig. S12). Quantitative RT-PCR revealed that *fgf receptor 1* (*fgfr1*) was expressed in the mesenchymal blastema rather than the regenerating nail epithelium (Supplementary Fig. S12). Consistently, phospho-ERK, a downstream mediator of FGF signaling, is detected in the Runx2$^+$ mesenchymal cells of control digits, but not in that of denervated digits and cKO digits (Supplementary Fig. S12). Similar defects in innervation and FGF2/p-ERK induction were observed upon deletion of *Wls* in K14$^+$ epithelial cells, causing failure in nail and digit regeneration (Supplementary Fig. S13). To test the function of FGF2 signal within blastema, we harvested blastema from control mice and allowed their outgrowth *in vitro*. Addition of FGF2 significantly enhanced the proliferation of blastema cells, while this effect is neutralized by RNA interference against *fgfr1* (Supplementary Fig. S14). Upon exposing blastema cells to bone differentiation media, alizarin red staining became positive, confirming their potential to differentiate into bone (Supplementary Fig. S14). Additionally, implantation of FGF2 soaked beads into denervated digits *in vivo* induced proliferation of Runx2$^+$ mesenchymal blastema, unlike that of control PBS soaked beads (Supplementary Fig. S14).

The above results suggest that Wnt activation in the nail epithelium performs dual functions to promote both nail regeneration and Runx2$^+$ mesenchymal cell growth through its ability to induce nerve-dependent FGF2 expression. We then asked why digits do not regenerate after amputations proximal to the nail (Supplementary Fig. S2). Careful examination of the amputated digits showed that amputations of the visible nail plate (i.e. removal of more than 50% of distal phalanx) do not remove the entire NSC region although it is known to fail in regeneration[10] (Supplementary Fig. S15). Unlike distal amputations that induce regeneration, these amputations within the NSC region removed the distal matrix expressing Wntless which is required for initiation of Wnt signaling (Supplementary Fig. S15). Consequently, these amputations failed to activate epithelial Wnt signaling, as revealed by the lack of nuclear β-catenin and TCF1 expression after re-epithelialization (Fig. 4b–c), resulting in the failure to regenerate the nail and digit (Fig. 4g, Supplementary Fig. S2).

To test whether stabilization of β-catenin in K14$^+$ epithelium, including the NSC region, can induce digit regeneration, we treated *K14-CreER;β-catenin$^{fl/ex3}$* mice with TAM following completion of re-epithelialization (Fig. 4a). One week after the initial TAM treatment, basal nail epithelial cells including NSC region exhibited nuclear β-catenin (Fig. 4b). In these tissues, NSC progeny expressed TCF1 as they regenerate distal matrix whereas the proximal end of the NSC region contained TCF1 negative cells (Fig. 4c). Although a transcriptional response to β-catenin stabilization was not directly evaluated, the spatially restricted pattern of TCF1 expression suggest that unidentified mechanisms may be present to cause the disparity in the activation of the pathway which acts downstream of β-catenin stabilization. Nevertheless, it was noteworthy that the regeneration of TCF1$^+$ distal nail matrix in these mutant mice accompanied the formation of a well-innervated blastema, which is never

observed in control mice upon amputation at this proximal level (Fig. 4d). Accordingly, we observed nail epithelial FGF2 expression and proliferating Runx2+mesenchymal cells, leading to digit bone regeneration (Fig. 4e–f, Supplementary Fig. S16). In these mice, nail regeneration was also grossly apparent and nails without amputations did not show any detectable changes (Fig. 4g, 4i, Supplementary Fig. 17). By contrast, when β-catenin stabilization was induced in K14+ skin epithelial cells after amputation proximal to the NSC region and subsequent re-epithelialization, neither TCF1 expression nor nail formation was observed (Supplementary Fig. S18). This suggests that the skin epidermis and NSCs respond differently upon β-catenin stabilization due to differences within the intrinsic lineage and/or underlying mesenchyme. Notably, Runx2+ cells and Sp7+ cells were found in the mesenchyme but did not show proliferative activity, resulting in the failure to regenerate the digit (Supplementary Fig. S18). These results show that the distally-restricted capacity of digit regeneration is partly due to insufficient Wnt induced signals/mechanisms in the nail epithelium, rather than an inherent absence of cells competent to regenerate the digit bone.

By demonstrating the presence of NSCs that undergo Wnt-dependent differentiation into the nail, we have uncovered a unique role of the nail epithelium in digit tip regeneration. Past studies in lower vertebrates have documented the vital roles of Wnt and FGF signaling in promoting limb regeneration[29,30]. These studies were limited by their inability to control gene expression in specific cell populations. We utilized epithelial-specific gene modification and demonstrated the function of epithelial Wnt signaling in digit tip, to open a new avenue to dissect epithelial-mesenchymal interactions that drive organ regeneration in mammals. The dual function of Wnt signaling in NSC lineage to direct nail formation and digit regeneration appears to be a key mechanism that coordinates regeneration of epithelial and mesenchymal tissues in mammalian digit tip regeneration (Supplementary Fig. S1). Further studies of mechanisms regulating NSCs and their interaction with mesenchymal cells may eventually lead to novel direction to treat amputees.

Method summary

All mice except β-catenin$^{(ex3)fl/+}$ mice were obtained from The Jackson Laboratory, and maintained in the Smilow Animal Facility at NYU. All animal protocols were approved by the IACUC at NYU School of Medicine. Cre recombination was induced by TAM injection as previously described[14]. Digit amputation, denervation and beads implantation was performed according to the previously reported method with modification[8]. Histology and histochemistry were performed on paraffin sections. For microarray analysis, basal cells of nail epithelium were isolated by FACS. Cells for colony forming assay were obtained by microdissection followed by enzymatic digestion. Statistical analyses were performed using Microsoft Excel.

Methods

Mice and sample collections

All mice except β-catenin $^{fl/ex3}$ mice[31] were obtained from Jackson Laboratories, and maintained in the Smilow Central Animal Facility at NYU Langone Medical Center. All animal protocols were approved by the IACUC at NYU School of Medicine. Cre

recombination in K14-CreER; Rosa$^{stop\text{-}LacZ}$ [32], K14-CreER; β-catenin $^{fl/fl}$ [33], K14-CreER; β-catenin $^{fl/ex3}$ and K14-CreER;Wntless$^{fl/fl}$ [34]mice was induced by TAM injection as published[14]. For nail sample collections, we sacrificed mice by CO_2 narcosis, and harvested the middle 3 digits of the hind limbs.

X-gal staining

Nail samples from K14-CreER; Rosa$^{stop\text{-}LacZ}$, Topgal[35] and Axin2-LacZ[36] mice were fixed in 4% PFA at 4 °C for 30 min, rinsed with PBS and incubated in X-gal (5-bromo-4-chloro-3-indolyl-β-d-galactopyranoside) solution as previously described[14]. After photographing X-gal stained whole mount nail samples under a dissection microscope (Zeiss, Discovery V12.), nail samples were incubated in 30% sucrose at 4 °C overnight, embedded into OCT-compound (Sakura), and cut into 10 μm thick frozen sections.

Immunohistochemistry

Nails were fixed in 10% Zinc buffered formalin at 4°C 2? Overnight [the meaning unclear; MMT], and washed in PBS twice. After decalcification in 22.5% formic acid/10% sodium citrate buffer at RT for 2 hr, nails were dehydrated through ethanol and xylene, embedded in paraffin, and cut into 6 μm sections. Following rehydration, paraffin-sectioned tissues were processed in hematoxylin and eosin, or Masson's trichrome staining. For immunohistochemistry, antigen retrieval was performed by microwaving sections for 6 min on high-wattage setting in 1x TE buffer (pH. 8.0). Sections were blocked in 10% fetal bovine serum (FBS)/PBS at RT for 1 hr, then incubated with primary antibodies against K14 (1:500, Covance), K17 (1:500, Abcam), AE13 (1:50, a gift of TT Sun, New York University), Ki67 (1:50, Abcam), Ctnnb1 (1;400, Sigma), Tcf1 (1:50, Cell signaling), Runx2 (1:100, Sigma), Sp7 (1:100, Santa Cruz)acetylated tubulin (1:500, Sigma), Fgf2 (1:100, Santa Cruz), pERK (1:100, Cell signaling; 1:20, Abcam) and Msx1 (1:20, Abcam) at 4 °C overnight, followed by incubation with fluorescein conjugated, or biotinylated secondary antibodies at RT for 2 hr. For biotinylated secondary antibodies, a third amplification step with streptavidin-conjugated TRITC (1:200, Vector) or Horseradish peroxidase (HRP, 1:500, Upstate) were performed. A diaminobenzidine (DAB) substrate solution (Sigma) was used for developing signals for HRP. All antibodies were diluted in 0.1% Triton-X 100/PBS.

Transmission electron microscopy

Samples were fixed in 0.1M sodium cacodylate buffer (pH 7.2) containing 2.5% glutaraldehyde, and 2% paraformaldehyde for 2 h at RT and 4 °C O/N. After post-fixation in 1% osmium tetroxide for 1.5 h at RT, samples were processed using standard methods and embedded in EMbed 812 (Electron Microscopy Sciences). Semi-thin sections were cut at 1 um and stained with 1% Toluidine Blue to evaluate the quality of preservation. Ultrathin sections (60 nm) were cut, mounted on copper grids and stained with uranyl acetate and lead citrate. Stained grids were examined under a Philips CM-12 electron microscope (FEI; Eindhoven, Netherlands) and photographed with a Gatan (4k ×2.7k) digital camera (Gatan, Inc.).

Whole-mount visualization of digit bone

Nails were fixed in 4% PFA at 4°C O/N. After washing in 1% KOH in H_2O, digits were incubated serially in 20% glycerol/1% KOH for 3–6 h at RT, 50% glycerol/1% KOH for 4 – 16 h at RT and 100% glycerol O/N at RT.

Immunocytochemistry

Dissociated cells were resuspended in 1% FBS/PBS and spun onto glass slides using Cytospin 3 (Shandon, Cheshire, UK). The slide was fixed with acetone at −20 °C for 10 min. Following washes in 1xPBS, slides were blocked in 10% fetal bovine serum (FBS)/PBS at RT for 1 h, then incubated with primary antibodies against K14 (1:500, Covance) at 4°C O/N, followed by incubation with AlexaFlor 488 conjugated secondary antibody at RT for 2 h. After washing in 1xPBS, slides were incubated with primary antibodies against K17 (1:5000, Abcam) at 4 °C O/N, and biotinylated secondary antibodies at RT for 2 h, and then streptavidin-labeled tetramethyl rhodamine isothiocyanate(SA-TRITC) (1:200, Vector) at RT for 1 h. Primary antibodies were diluted in 10% FBS/PBS, and secondary antibodies were diluted in PBS.

Colony forming assay

Thirty nails from at least 5 different mice (8–10 week-old FVB mice) were collected, and the nail fold overhanging the nail plate was removed with surgical blades and forceps under a dissection microscope. Dissected fragments were incubated in 0.25% Trypsin for 1 h 45 min at 37 °C, and then in 0.35% Collagenase I and DNase I for 10 min each at 37 °C. Dissociated cells were resuspended in DMEM/10% FBS. The percentage of $K14^+$ cells was then determined by cytospin analysis as described below. Cell suspensions containing 1×10^4 $K14^+$ cells were cultured with NIH/3T3 feeder layers (a gift from Dr. Alka Mansukhani, New York University) in F10: DMEM (1:3) media with 10% new born calf serum in 6-well plates[37]. After 14 days in culture, cells were fixed with 10% buffered formalin and stained with 1% Rhodamine B. The number of colonies was manually counted and the size of the colonies was measured using image analysis software (Image J, NIH), and colony forming efficiency (the number of colonies larger than 3 $mm^2/1\times10^4$ cells) was calculated. Studies were performed three independent times.

Gene expression profiling of NSCs by microarray

7–8 week-old K14-rtTA; TetO-H2B-GFP mice (Jackson Laboratory) were treated with Dox for 7 d to label the entire $K14^+$ matrix cells with GFP. Thirty digits from at least 5 different mice were collected and single cell suspensions were prepared as described above. The cells were incubated with APC conjugated anti-CD49f antibody in 1% FBS/PBS, for 15 min at RT. Basal nail epithelial cells from each fraction were isolated using FACS based on the GFP label, representing K14 positivity, and expression of CD49f, a general marker of basal cells. To obtain sufficient cells for oligonucleotide gene chip hybridization, we used the Ovation RNA Amplification System V2 (Nugen) for mRNA amplification. The amplified mRNA was labeled and hybridized to the Mouse 430.2 microarrays (Affymetrix). Data was analyzed with GeneSpring X software, and genes that were differentially regulated at least 2

fold were selected for further analysis. GEO accession numbers; GSE45494, GSM1105640, GSM1105641, GSM1105642 and GSM1105643.

Digit amputation

Digit amputation was performed according to the previously reported method with modification[8]. Briefly, the central three digits (digit 2, 3 and 4) of hind limbs of 21 days old mice were amputated at the level of the middle of nail matrix or in NSCs area. Amputated digits were collected at 1, 2, 3 and 5 weeks after amputation, and processed for Alucian blue/Alizarin red or immunohistochemistry. More than 10 different digits from 5 mice were used for each time point. Studies were repeated three times.

In situ hybridization

Digoxigenin-labeled RNA probes complementary to *Bmp4* (a gift of Han M and Muneoka K, Tulane University) were synthesized according to manufacturer's instructions (DIG-RNA Labeling Kit, Roche). *In situ* hybridization was performed using previously described method[14]. Studies were repeated three times.

Denervation

The sciatica nerve of 2-week-old mice was approached through a rectilinear longitudinal cutaneous incision on the lateral surface of the right thigh, and a 3–5 mm segment was removed. The wound was closed with surgical staple. Digits were amputated at 1 week after denervation. Amputated digits were collected at 1, 2, 3, 4 and 5 weeks after amputation. More than 10 different digits from 5 mice were used for each time point. Studies were repeated with 3 different litters.

Blastema cell culture and bone differentiation assay

Digit tip proximal to the terminal phalanx was collected at 3 w after digit amputation. Mesenchymal blastema cell mass was separated from the nail epidermis by sine forceps and needle under the dissecting microscope. Isolated blastema cell mass was placed in 24-well plate with DMEM (invitrogen)/10% FBS (Cellgro), and incubated at 37 °C, 5 % CO_2. After 1w in culture, blastem cells were transfected with 50nM siRNA against for *FGFR1* (Invitrogen, MSS204294 and MSS204295) or control siRNA, using Lipofectamine RNAiMAX (Invitrogen). Transfected cells were incubated in DMEM (invitrogen)/10% FBS (Cellgro) with or without 20ng/ml FGF2 (Sigm-Aldrich) at 37°C, 5% CO_2 for 2 d, and were stained for Ki67 as described above. For bone differentiation assay, culture media was replaced with HyClone® Advance STEM™ Osteogenesis differentiation medium (Thermo Scientific) at 7 days in culture. After 3 w in culture, mineralization was assessed by alizarin red staining. In brief, the cultures were fixed in 10% Zinc buffered formalin at RT for 10 min, wash in PBS twice, and stained with 2% alizarin red S (Sigma) in distilled water for 5 min at RT. The stained cell layers were washed, rinsed twice with distilled water, and air-dried.

Beads implantation

We performed bead implantation experiment using previously described method (Yu et al., 2010) with the following modifications. Briefly, Affi-Gel Blue Gel beads (Bio-Rad) were washed with 0.1% BSA/PBS then soaked with recombinant human Fgf2 (Sigma) at a concentration of 0.3 mg/ml or 0.1% BSA/PBS as a control for 2 hours at room temperature. Beads implantation was performed at 2 weeks after digit amputation after the completion of wound closure was confirmed.

Statistical analysis

Student's t-test was used to calculate p-values on Microsoft Excel, with two-tailed tests and unequal variance.

Supplementary Material

Refer to Web version on PubMed Central for supplementary material.

Acknowledgments

We thank Drs. T. Andl, T. Endo, L. Miller, P. Myung, M. Schober, and T.T. Sun for invaluable suggestions and discussion. We thank Dr. T. Endo for demonstrating the method of beads implantation. We thank Dr. T.T. Sun for the AE13 antibody, Dr. K. Muneoka for *Bmp4* plasmid, Dr. A. Mansukhani for NIH/3T3 cells. We thank the Genome Technology Center at NYU (NIH grant 5P30CA0016087-32 and P30 CA016087-30), and the Center for Functional Genomics at University at Albany for performing microarray. We thank Dr. F. Liang at NYU Microscopy Core for TEM analysis. We thank NYU Microscopy Core of for use of confocal microscope (NCRRS10 RR023704-01A1). M.T is supported by NYU Kimmel Stem Cell Center and NYSTEM training grant C026880. M.I. is supported by NIH/NIAMS grant 1R01AR059768-01A1, Ellison Medical Foundation and funding from Department of Dermatology and Cell Biology, and the Helen and Martin Kimmel Center for Stem Cell Biology at NYU.

References

1. Douglas BS. Conservative management of guillotine amputation of the finger in children. Aust Paediatr J. 1972; 8:86–89. [PubMed: 5074173]
2. Borgens RB. Mice regrow the tips of their foretoes. Science. 1982; 217:747–750. [PubMed: 7100922]
3. Zhao W, Neufeld DA. Bone regrowth in young mice stimulated by nail organ. J Exp Zool. 1995; 271:155–159.10.1002/jez.1402710212 [PubMed: 7884389]
4. Mohammad KS, Day FA, Neufeld DA. Bone growth is induced by nail transplantation in amputated proximal phalanges. Calcif Tissue Int. 1999; 65:408–410. [PubMed: 10541769]
5. Rinkevich Y, Lindau P, Ueno H, Longaker MT, Weissman IL. Germ-layer and lineage-restricted stem/progenitors regenerate the mouse digit tip. Nature. 2011; 476:409–413.10.1038/nature10346 [PubMed: 21866153]
6. Lehoczky JA, Robert B, Tabin CJ. Mouse digit tip regeneration is mediated by fate-restricted progenitor cells. Proc Natl Acad Sci U S A. 2011; 108:20609–20614.10.1073/pnas.1118017108 [PubMed: 22143790]
7. Neufeld DA. Partial blastema formation after amputation in adult mice. J Exp Zool. 1980; 212:31–36.10.1002/jez.1402120105 [PubMed: 7411075]
8. Han M, Yang X, Lee J, Allan CH, Muneoka K. Development and regeneration of the neonatal digit tip in mice. Dev Biol. 2008; 315:125–135.10.1016/j.ydbio.2007.12.025 [PubMed: 18234177]
9. Neufeld DA, Zhao W. Phalangeal regrowth in rodents: postamputational bone regrowth depends upon the level of amputation. Prog Clin Biol Res. 1993; 383A:243–252. [PubMed: 8302899]

10. Norton LA. Incorporation of thymidine-methyl-H3 and glycine-2-H3 in the nail matrix and bed of humans. J Invest Dermatol. 1971; 56:61–68. [PubMed: 5556500]
11. Fleckman P, Jaeger K, Silva KA, Sundberg JP. Comparative anatomy of mouse and human nail units. Anat Rec (Hoboken). 2013; 296:521–532. [PubMed: 23408541]
12. Al-Qattan MM. WNT pathways and upper limb anomalies. J Hand Surg Eur Vol. 2011; 36:9–22.10.1177/1753193410380502 [PubMed: 20709709]
13. Blaydon DC, et al. The gene encoding R-spondin 4 (RSPO4), a secreted protein implicated in Wnt signaling, is mutated in inherited anonychia. Nat Genet. 2006; 38:1245–1247.10.1038/ng1883 [PubMed: 17041604]
14. Adaimy L, et al. Mutation in WNT10A is associated with an autosomal recessive ectodermal dysplasia: the odonto-onycho-dermal dysplasia. Am J Hum Genet. 2007; 81:821–828.10.1086/520064 [PubMed: 17847007]
15. Rabbani P, et al. Coordinated activation of Wnt in epithelial and melanocyte stem cells initiates pigmented hair regeneration. Cell. 2011; 145:941–955.10.1016/j.cell.2011.05.004 [PubMed: 21663796]
16. Al Alam D, et al. Contrasting expression of canonical Wnt signaling reporters TOPGAL, BATGAL and Axin2(LacZ) during murine lung development and repair. PLoS One. 2011; 6:e23139.10.1371/journal.pone.0023139 [PubMed: 21858009]
17. Lin MH, Kopan R. Long-range, nonautonomous effects of activated Notch1 on tissue homeostasis in the nail. Dev Biol. 2003; 263:343–359. [PubMed: 14597207]
18. Nakamura M, Ishikawa O. The localization of label-retaining cells in mouse nails. J Invest Dermatol. 2008; 128:728–730.10.1038/sj.jid.5701062 [PubMed: 17914453]
19. van de Wetering M. Armadillo coactivates transcription driven by the product of the Drosophila segment polarity gene dTCF. Cell. 1997; 88:789–799. [PubMed: 9118222]
20. Banziger C, et al. Wntless, a conserved membrane protein dedicated to the secretion of Wnt proteins from signaling cells. Cell. 2006; 125:509–522.10.1016/j.cell.2006.02.049 [PubMed: 16678095]
21. Zhou P, Byrne C, Jacobs J, Fuchs E. Lymphoid enhancer factor 1 directs hair follicle patterning and epithelial cell fate. Genes Dev. 1995; 9:700–713. [PubMed: 7537238]
22. Lynch MH, O'Guin WM, Hardy C, Mak L, Sun TT. Acidic and basic hair/nail ("hard") keratins: their colocalization in upper cortical and cuticle cells of the human hair follicle and their relationship to "soft" keratins. J Cell Biol. 1986; 103:2593–2606. [PubMed: 2432071]
23. Ducy P, Zhang R, Geoffroy V, Ridall AL, Karsenty G. Osf2/Cbfa1: a transcriptional activator of osteoblast differentiation. Cell. 1997; 89:747–754. [PubMed: 9182762]
24. Mohammad KS, Neufeld DA. Denervation retards but does not prevent toetip regeneration. Wound Repair Regen. 2000; 8:277–281. [PubMed: 11013019]
25. Brockes JP. The nerve dependence of amphibian limb regeneration. J Exp Biol. 1987; 132:79–91. [PubMed: 3323408]
26. Kantor DB, et al. Semaphorin 5A is a bifunctional axon guidance cue regulated by heparan and chondroitin sulfate proteoglycans. Neuron. 2004; 44:961–975.10.1016/j.neuron.2004.12.002 [PubMed: 15603739]
27. Zhang Y, et al. Activation of beta-catenin signaling programs embryonic epidermis to hair follicle fate. Development. 2008; 135:2161–2172.10.1242/dev.017459 [PubMed: 18480165]
28. Mullen LM, Bryant SV, Torok MA, Blumberg B, Gardiner DM. Nerve dependency of regeneration: the role of Distal-less and FGF signaling in amphibian limb regeneration. Development. 1996; 122:3487–3497. [PubMed: 8951064]
29. Kawakami Y, et al. Wnt/beta-catenin signaling regulates vertebrate limb regeneration. Genes Dev. 2006; 20:3232–3237.10.1101/gad.1475106 [PubMed: 17114576]
30. Yokoyama H, Ogino H, Stoick-Cooper CL, Grainger RM, Moon RT. Wnt/beta-catenin signaling has an essential role in the initiation of limb regeneration. Dev Biol. 2007; 306:170–178.10.1016/j.ydbio.2007.03.014 [PubMed: 17442299]
31. Harada N, et al. Intestinal polyposis in mice with a dominant stable mutation of the beta-catenin gene. Embo J. 1999; 18:5931–5942.10.1093/emboj/18.21.5931 [PubMed: 10545105]

32. Vasioukhin V, Degenstein L, Wise B, Fuchs E. The magical touch: genome targeting in epidermal stem cells induced by tamoxifen application to mouse skin. Proc Natl Acad Sci U S A. 1999; 96:8551–8556. [PubMed: 10411913]

33. Lowry WE, et al. Defining the impact of beta-catenin/Tcf transactivation on epithelial stem cells. Genes Dev. 2005; 19:1596–1611.10.1101/gad.1324905 [PubMed: 15961525]

34. Myung PS, Takeo M, Ito M, Atit RP. Epithelial Wnt Ligand Secretion Is Required for Adult Hair Follicle Growth and Regeneration. J Invest Dermatol. 201210.1038/jid.2012.230

35. DasGupta R, Fuchs E. Multiple roles for activated LEF/TCF transcription complexes during hair follicle development and differentiation. Development. 1999; 126:4557–4568. [PubMed: 10498690]

36. Lustig B, et al. Negative feedback loop of Wnt signaling through upregulation of conductin/axin2 in colorectal and liver tumors. Mol Cell Biol. 2002; 22:1184–1193. [PubMed: 11809809]

37. Barrandon Y, Green H. Three clonal types of keratinocyte with different capacities for multiplication. Proc Natl Acad Sci USA. 1987; 84:2302–2306. [PubMed: 2436229]

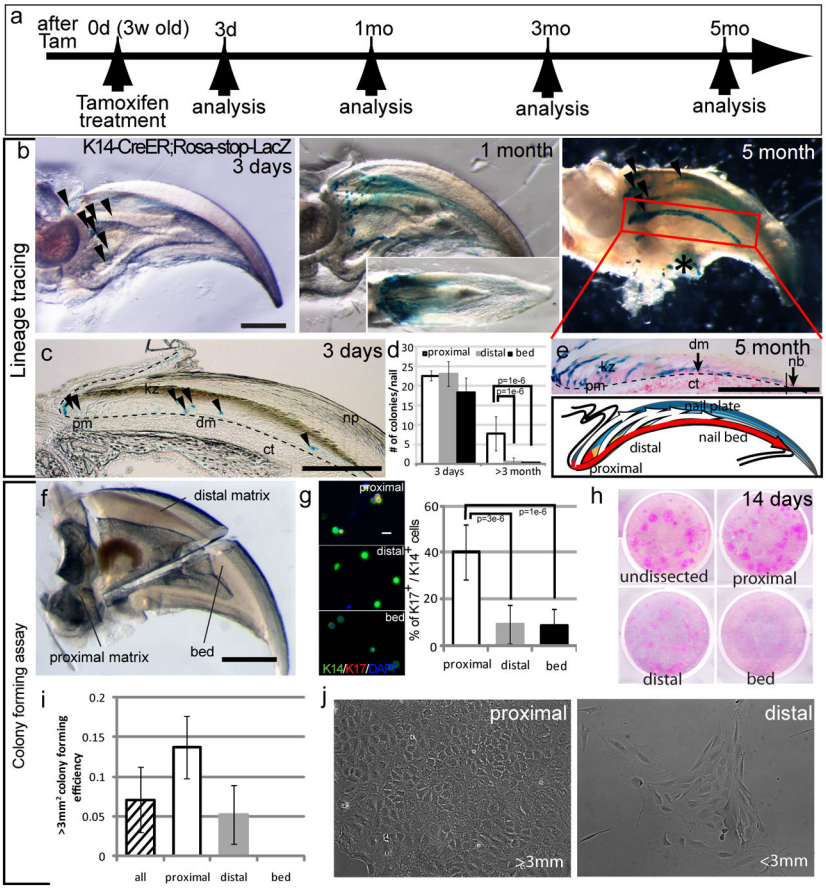

Fig. 1. NSCs are harbored in the proximal nail matrix

a. Experimental scheme. **B, c.** Whole mount (b) and sectioned (c) specimens of K14-CreER;R26R reporter mice. LacZ expression was detected at indicated times after TAM treatment. Inset in (b) shows top view of the nail. **d,** Quantitative analysis of LacZ positive streaks. **e,** Tissue section analysis of a $LacZ^+$ colony at 5 mo after chase and schematic representation, to illustrate cell lineages from proximal matrix cells. **f.** A typical nail sample used for microdissection to obtain proximal, distal and bed fragments. **g,** Immunocytochemistry for K14 and K17 using single cell suspensions from each compartment. **h–j,** *In vitro* colony forming assay with single cell suspensions obtained from indicated fragments. Visualization of colonies by Rhodamine B staining (h) and quantification of colonies >3 mm^2 (i). Brightfield images of proximal and distal nail epithelial colonies (j). Arrowheads indicate $LacZ^+$ cell or colony. Dashed lines delineate the boundary between nail epithelium and underlying connective tissue (ct). Asterisk indicates nonspecific background. Data are presented as the mean ± SD. Scale bars, 500 μm in (b and f); 100 μm in (c and e). dm, distal matrix, kz, keratogenous zone, nb, nail bed, np, nail plate, pm, proximal matrix.

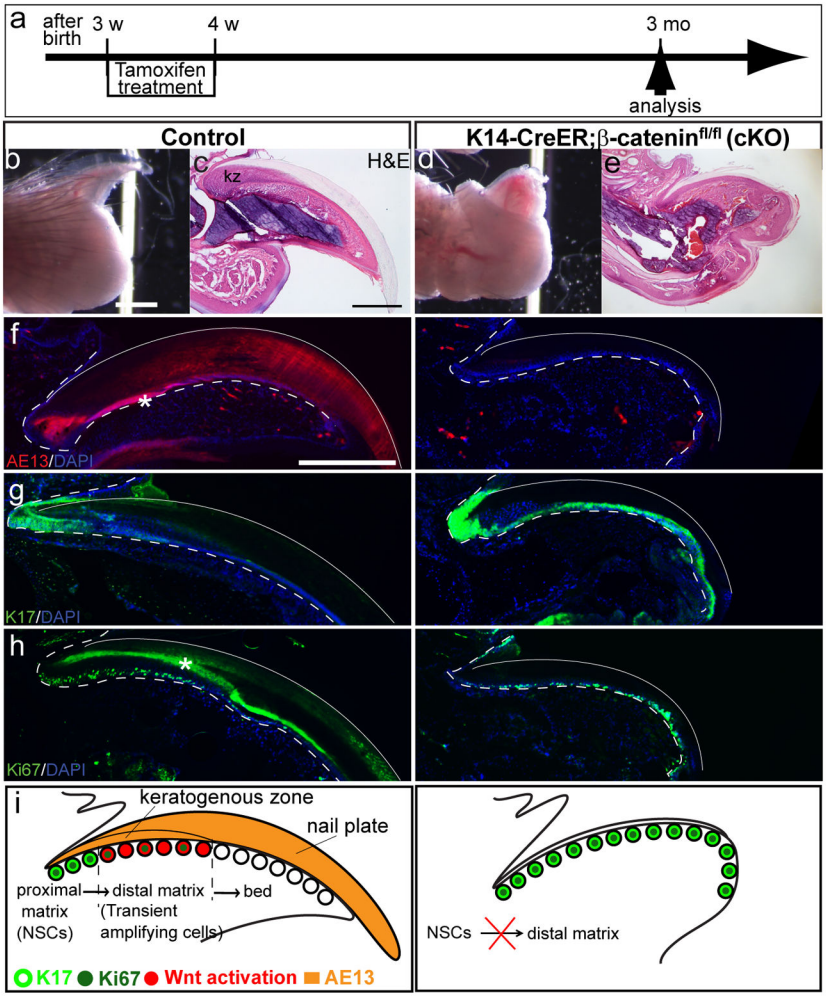

Fig. 2. Epithelial β-catenin is required for nail differentiation

a. Experimental scheme. Three-week-old K14-CreER; β-catenin cKO mice and littermates were treated with TAM for 7 d, and analyzed at 2 mo after TAM treatment. **b–e.** Gross appearance (b and d) and H&E staining (c and e) of control (b and c) and cKO digit (d and e). **f–h.** Immunofluorescence for indicated markers at 2 mo after TAM treatment. **i**. Summary of immunohistochemistry in (f–h). Dashed lines indicate the border between nail basal layer and connective tissue. Lines indicate the outline of nail plate in (f–h). Asterisks show nonspecific background. Scale bars, 500 μm in (b, c and f).

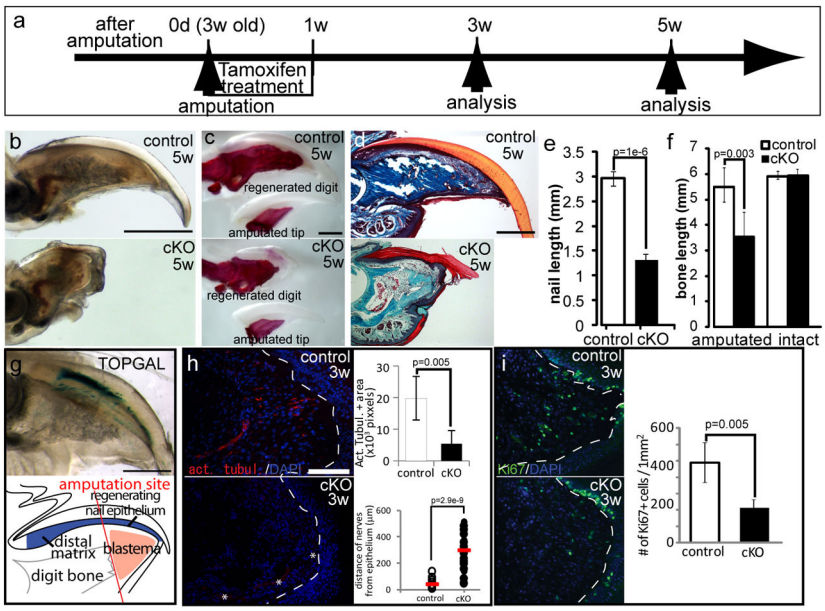

Fig. 3. Nail epithelial β-catenin is required for blastema growth and digit regeneration

a. Experimental scheme. Three-week-old old K14-CreER;β-catenin cKO mice and littermates were treated with TAM for 7 d immediately after distal tip amputation, and analyzed at the indicated time points. **b,** Gross appearance of regenerated digit at 5 w after amputation. **c.** Whole mount alizarin red analysis. **d.** Trichrome staining. **e and f.** Quantification analyses of the nail length (h) and the bone length (i) at 5 w after amputation. **g.** Analysis of Wnt activation in regenerating nail epithelium using TOPGAL at 3 w after amputation. Lower panel is the schematic illustration of the upper panel. **h.** Quantitative analyses of the distance between nerve tip and wound epidermis and the innervations at 3w after amputation. **i.** Proliferation analyses by Ki67 immunohystochemistry at 3w after amputation. Red bar in o indicates the average. Dashed lines, border between nail epithelium and connective tissue. Arrows Asterisks in (n, o and r) indicate autofluorescence from blood cells. Data are presented as the mean ± SD. Scale bars, 500 μm in (b–d); 100 μm in (h).

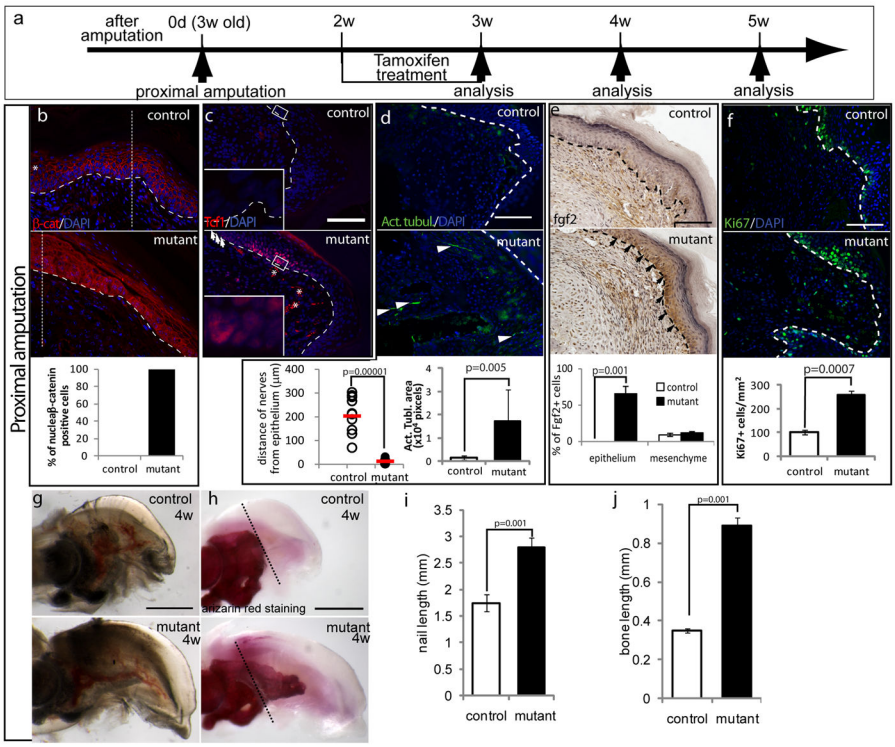

Fig. 4. Forced Wnt activation in wound epidermis can overcome the limitation of regeneration following proximal amputation

a. Experimental scheme. Three-week-old K14-CreER;β-catenin$^{fl/ex3}$ (mutant) mice and littermate controls were treated with TAM for 7 days starting from 2 w after amputation at the proximal level. **b–f,** Immunohistochemical analyses with indicated markers at 3 w after amputation. **g and,** Gross appearance of regenerated digits. **h,** Whole mount alizarin red analysis. **i and j,** Quantification analyses of the nail (i) and bone length (j) at 4 w after amputation. Red bars in n show the meal values. Arrows in (c) and (e) indicate Tcf1^{-} proximal matrix and FGF2^{+} epidermis, respectively. Arrowheads in d point nerves. Dotted lines in b, c, g and h indicates amputation plane. Dashed lines indicate the border between epidermis and connective tissue. Dotted lines in (b) indicate amputation planes. Quantified data are presented as the mean ± SD. Scale bar, 100 μm in (b–f), 500 μm in (g and h).